Design and Characterization of a Micro-scale Calorimetric Flow Rate Sensor for Sweat Hydration Detection

Che Ting Ho, Ahmed Tashfin Iftekhar, and Dr.Tolga Kaya
School of Engineering and Technology
Central Michigan University
Mount Pleasant, MI 48859
Email: ho1c@cmich.edu iftek1a@cmich.edu kaya2t@cmich.edu

Abstract

Studying sweat and its contents can reveal important information regarding human physiology. Although sweat conductivity is a good indication for hydration status, it is known that the sweat rate affects the sweat concentration hence the conductivity. Therefore, sweat rate detection would help further assess the sweat conductivity. Here, a micro-scale calorimetric flow meter was discussed for measuring sweat flow rate that is on the order of 2µL/min ± 0.1µL. A numerical model for the sweat flow rate sensor has been developed in MATLAB. Finite element analysis simulations were carried out using COMSOL Multiphysics. Our results showed that the sensitivity is a strong function of the distance between the heater and sensors along with the dimension of the channel. Moreover, having the sensors on platforms would increase the sensitivity of the device.

Introduction

Athletes and solders are constantly pushing themselves to perform physical activities during trainings or out in the fields and one major concern of their activities is their hydration level. If a person loses 1-2% of his/her bodyweight (BW) during exercise, it causes degradation in physiological and mental functions [1]. BW loses of more than 3% increases the risk of serious injuries such as heart problems and heart stroke. Currently, blood serum analysis is considered to be the gold standard method of measuring electrolyte concentrations. However, this technique is invasive and impractical for real-time, on-the-field assessment of hydration during competition [2, 3]. With its ease of accessibility and relatively strong electrolyte concentrations, sweat has drawn the attention as a real-time, non-invasive method for detection of hydration level [4-6].

Sweat compound sensing has mainly been studied using electrochemical measurement methods and historically started in the 1950s with sweat conductivity measurements for children who were diagnosed with Cystic Fibrosis [7, 8]. Electrochemical reactions with sweat on a set of electrodes are detected in terms of impedance change which is then correlated to the concentration of sweat. However, sweat electrolyte level detection itself does not provide sufficient data on one's hydration status. As the sweat rate increases, electrolyte reabsorption in the sweat gland ducts decreases leading to increased electrolyte loss with sweating [9-11]. Recently, engineers have begun to develop continuous sweat rate sensors based on micromachined hygrometers and capacitive sweat absorbers [12, 13]. The use of humidity sensors or image analysis for the detection of sweat rate has also been reported [13, 14, 15]. In addition, it was widely accepted that microflow sensing (flow rates around μL/min) is implemented with thermal flow rate sensors particularly calorimetric or thermal pulse flow sensors [16-19]. In this study, we investigated the performance of a calorimetric sensor design for sweat rate detection based on theoretical calculations and finite element analysis simulations using MATLAB and COMSOL Multiphysics. The results revealed the potential of calorimetric flow rate sensors as an implementation for electrochemical sweat sensors.

Device Design

Calorimetric flow meter design shown in Fig. 1 has a heating element and two temperature sensors, namely upstream and downstream sensors, with respect to the heater. The downstream temperature sensor's readings would be dependent on the flow rate as higher flow rate would cause the temperature cool down and create temperature difference between to temperature sensors. Heat transfer in fluids is utilized to determine the flow rate of the liquid flow [17]. Heat conduction and heat convection take place in the channel in both axes. The heating element and sensors are placed at the bottom of the channel as shown in Fig. 1. The heating element consists of an array of four heaters modeled as copper, each with a height of 100 nm and a length of 100 μm. The heaters are spaced evenly by 100 μm. Sensors are modeled as copper electrodes with the same dimensions as each individual heater. The channel (25 mm × 1 mm × 1 mm) is foreseen to be created using soft lithography techniques by using polydimethylsiloxane (PDMS), a polymer widely used in microfluidic devices. Sweat can be collected from the skin and introduced to the channel through the tubing on the left in Fig. 1. Sweat inside the channel will be heated by the heater, and the temperature will be measured by the two sensors. The difference in temperature will be used to determine one's sweat rate.

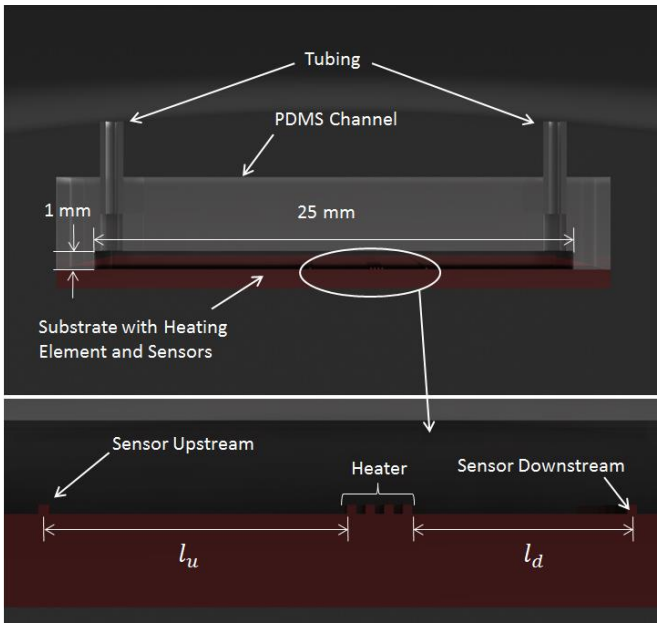

Figure 1. Schematic of the calorimetric flow meter. Temperature sensors are placed both sides of the heater to measure the temperature difference as a result of the rate of sweat flow.

Heat Transfer

The conservation of heat energy in the one dimensional model of the channel can be expressed as

$$P_{cond,x,fluid} + P_{conv,x,fluid} + P_{cond,x,Cu} = P_{cond,y,fluid} \quad (1)$$

The heat transfer continues until there is a thermal equilibrium. Conduction takes places both in the copper and fluid in the both axis but the convection takes places only for the fluid in x axis. Heat conduction for the fluid is expressed in terms of rate equation, fluid conductivity, λ_{Fl}, and the boundary layer height, δ, and the heater width, b_H, as

$$-\lambda_{Fl}\frac{T(x)}{2dx}b_H\delta \quad (2)$$

The heat conduction in the copper is given as the function of rate equation, heater width , b_H,and the diaphragm thickness, d_M, as

$$-\lambda_{Cu}\frac{T(x)}{dx}b_H d_M \quad (3)$$

The heat convection occurs in the fluid when thermal energy is transferred from hot places to the cool places in the channel and it is expressed in terms of fluid density, ρ_{Fl}, Thermal diffusivity a_{Fl}, flow rate v, as

$$\rho_{Fl}a_{Fl}v\frac{T(x)}{2} \quad (4)$$

And the fluid's conduction along the y axis is

$$\lambda_{Fl}\frac{T(x)}{\delta}b_H dx \quad (5)$$

The heat balance equation of the channel is the combination of Equation (2)-(5) and is given as below [20]

$$-\lambda_{Fl}\frac{T(x)}{2dx}b_H\delta + \rho_{Fl}a_{Fl}v\frac{T(x)}{2} - \lambda_{Cu}\frac{T(x)}{dx}b_H d_M = \lambda_{Fl}\frac{T(x)}{\delta}b_H dx \quad (6)$$

After differentiating the whole equation and dividing it by $\lambda_{Fl} b_H \delta$,

$$-\frac{1}{2}\frac{d^2T(x)}{dx^2} + \frac{\rho_{Fl} c_{Fl} v}{2\lambda_{Fl} b_H \delta}\frac{dT(x)}{dx} - \frac{\lambda_{Cu}\, d_M}{\lambda_{Fl}\,\delta}\frac{d^2T(x)}{dx^2} = \frac{T(x)}{\delta^2} \quad (7)$$

Thermal diffusivity is $a_{Fl} = \frac{\lambda_{Fl}}{\rho_{Fl} c_{Fl}}$, so from Equation (7)

$$\left(\frac{1}{2} + \frac{\lambda_{Cu}\, d_M}{\lambda_{Fl}\,\delta}\right)\frac{d^2T(x)}{dx^2} - \frac{v}{2a_{Fl}}\frac{dT(x)}{dx} - \frac{T(x)}{\delta^2} = 0 \quad (8)$$

Assuming,

$$a = \frac{1}{2} + \frac{\lambda_{Cu}\, d_M}{\lambda_{Fl}\,\delta},\ b = \frac{v}{2a_{Fl}},\ c = \frac{1}{\delta^2} \quad (9)$$

We know, Euler's equation,

$$y = Ae^{T(x)t} + Be^{-T(x)t} \quad (10)$$

Taking first and second order derivative, solving second order differential equation and by substituting Equation (9) we will get a simplified equation. The heat dissipation rate, γ, gets decreased exponentially to zero, as the distance between downstream sensor and the heater increases.

Considering, $k = \frac{1}{2} + \frac{\lambda_{Cu}\, d_M}{\lambda_{Fl}\,\delta}$, as a dimensionless factor, we will get Equation (11).

$$\gamma_{1,2} = \frac{v \pm \sqrt{v^2 + \frac{16 a_{Fl}{}^2 k}{\delta^2}}}{4 a_{Fl} k} \quad (11)$$

Finally, temperature difference between the two sensors [21],

$$T = T_0\left[e^{\gamma_2 l_u} - e^{-\gamma_1 l_d}\right] \quad (12)$$

Where, T_0= Heater temperature with respect to the room temperature
l_u=length between upstream sensor and the heater
l_d= length between downstream sensor and the heater

Considering the thermal diffusivity of sweat, neglecting the heat conduction in the silicon diaphragm $k = \frac{1}{2}$ [21] and also assuming for liquids with a small Reynolds number, $\delta = h$ it is possible to find out the value of $\gamma_{1,2}$ for different flow velocities and different temperature.

Numerical Simulations

The COMSOL model was similar to the device design mentioned before, where the channel and heater dimension remained the same and same distance was used for l_u and l_d, and had two temperature boundary conditions. With the thermal insulation of the PDMS channel and the substrate, the outer boundary temperature is essentially room temperature. Therefore, the boundary condition of the outer boundary of the channel was 293 K. Another boundary condition was needed to setup the heater temperature (330 K). When sensors are close to the boundary layer, both sensors would measure a temperature close to 293 K, which the temperature change is essentially 0 K. A platform (potentially to be fabricated using SU-8) was used to increase temperature difference between the two sensors. The height of the SU-8 layer used for initial trials was 100 μm, the heater and the sensors were 100 nm and placed on top of the SU-8 layer.

So, technically the sensor's height considering the SU8's height was 100.1 µm. The fluid material was water and the heater material was copper. Two physics had been selected, namely, heat transfer in fluid and laminar flow for the COMSOL model. Water was used as the liquid in the simulations. The range of the volumetric water flow for this model was 0-2 µL/min to represent the real human sweat rate [6]. For no flow condition in the channel, the temperature was distributed evenly. With the change of the flow, the temperature distribution changed along with higher flow towards the outlet as shown in Fig. 2.

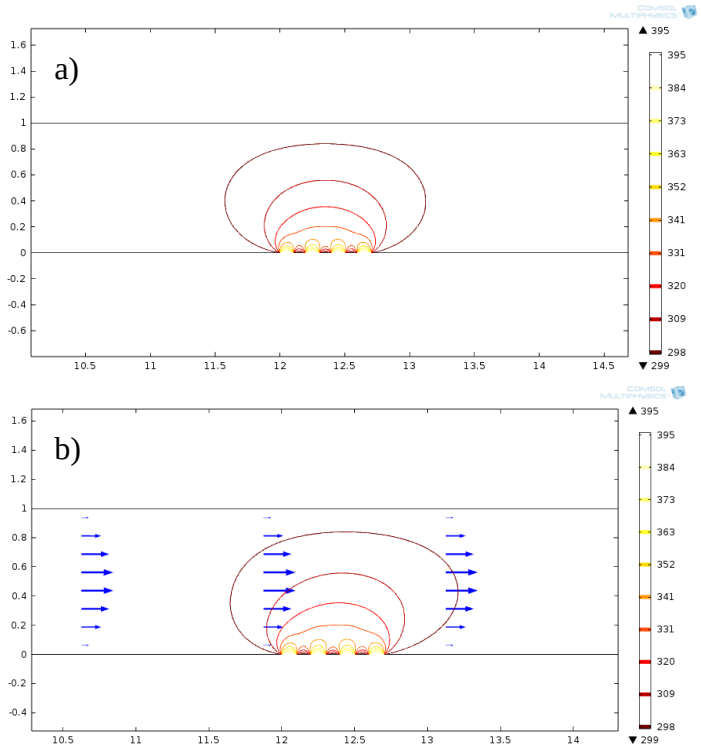

Figure 2. Temperature Distribution inside the channel with a) no flow and b) an inlet flow of 0.1 mm/s. Temperature is distributed evenly with no flow inside the channel and can be seen shifted along the direction of the flow when an inlet flow is presented.

A MATLAB code was created based on Equations (11) and (12) mentioned in the previous section. With our channel's dimensions, materials properties, and a predefined l_u and l_d, we calculated that the difference in temperature increases as the flow rate increase from 0 to 2 µL/min. The relationships between temperature difference and flow rate for both MATLAB calculations and COMSOL simulations were then compared in Fig. 3. The solid line in Fig. 3 represents MATLAB calculations and shows the relationship between the temperature difference at l_u and l_d and the flow rate. Although the channel used in COMSOL contained the SU-8 platforms and the one used in MATLAB calculations did not, both reserve the same positive trend and zero offset due to the asymmetrical l_u and l_d. As shown in Fig. 3, the temperature difference in COMSOL, presented in dotted line, was less than the results from MATLAB, which points out that the geometry of the channel and positions of the sensor have immense effect on the temperature difference between two sensors.

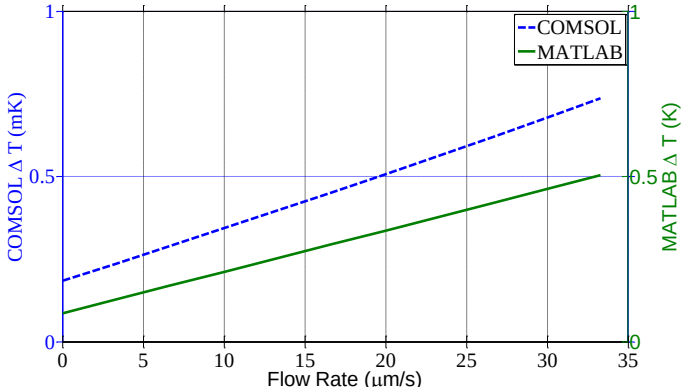

Figure 3. Positive, linear relationship between the difference in temperature and sweat rate plotted in MATLAB to compare COMSOL model and theoretical calculations. The dashed line was plotted according to the results from our COMSOL model, and the solid line was plotted using the Equations (11) and (12).

The dimensions of channel and positions of the downstream sensor were investigated. We compared the difference in temperature with the change of height and width of channel, where height and width equaled to each other and varied between 1-10 mm. The position of the sensors remained the same as what was used before in our COMSOL model that was used to determine the relationship between flow rate and temperature difference. While the volumetric flow rate flows in a range of 0-2 μL/min, the fluid velocity varied for each different cross-sectional area. We tested the change in cross-sectional area with three different heater temperature, 330 K, 360 K, and 400 K. Although a higher flow velocity, where the channel has the smallest cross-sectional area, was predicted to yield a larger difference in temperature, Fig. 4 shows that the maximum temperature difference occurs when both height and width were around 3-4 mm. Higher heater temperature resulted in greater temperature difference between the two sensors; however, the maximum point for each curve was still between 3-4 mm for the channel height and width.

The sensors' positions were then studied with a channel size of 25 mm x 1 mm x 1 mm. In terms of x-direction (direction along the flow inside channel), we considered keeping l_u at the same position as a reference point while l_d changes. l_u remained 2.95 mm away from the heater and on a 100 μm platform. l_d varied in x-direction and was on a 100 μm as well. Fig. 5 shows a schematic of the change in position and platform height. As shown in Fig. 6a, a smaller l_d yielded greater change in temperature. This temperature difference decayed exponentially as the downstream sensor moved further away from the heating element. In Fig. 6b, we compared the temperature difference with difference platform heights for three different distances between the sensor and heater, 0.5 mm, 1 mm, and 1.2 mm. The platform height of both upstream and downstream sensors was the same and varied between 0-0.7 mm.

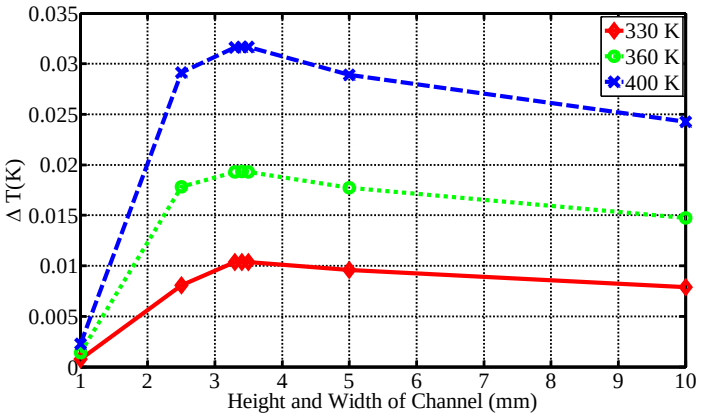

Figure 4. Temperature difference with differnet dimensions for channel height and width, where their dimensions are the same.

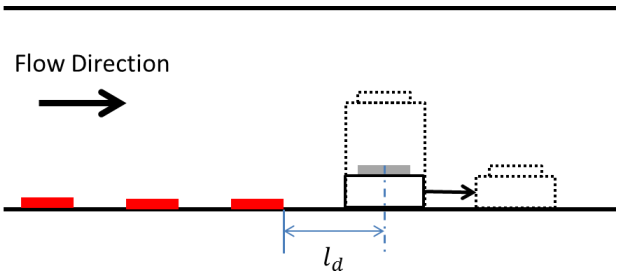

Figure 5. Schematic of changing the x and y position of the sensor by moving the platform or increasing the platform height.

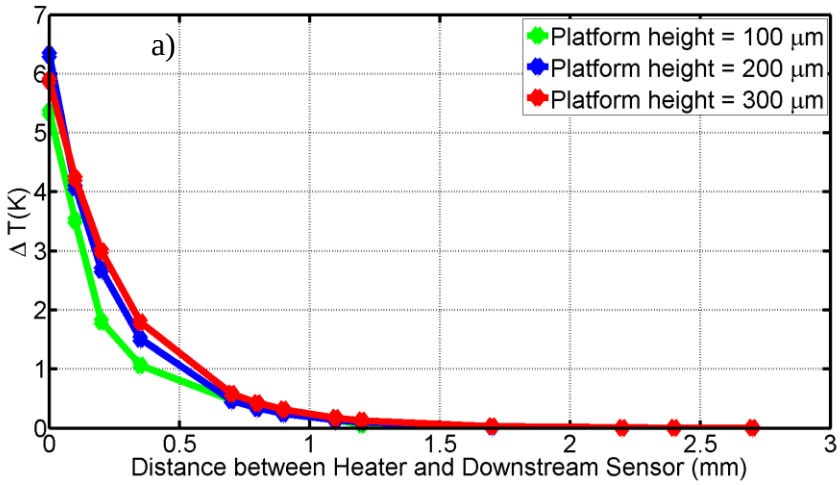

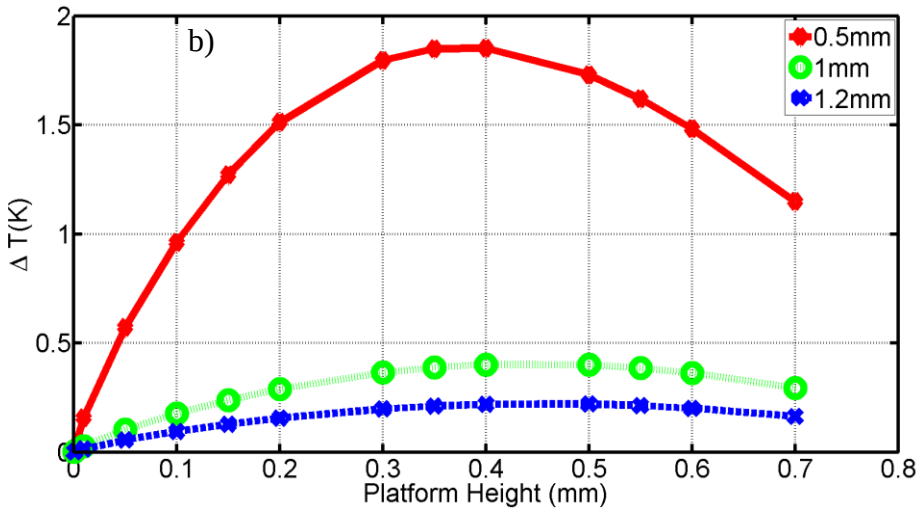

Figure 6. Temperature difference of a) different distance away from the heater at 3 different platform heights and b) different platform heights at 3 different l_d for downstream sensor.

Conclusion

This study pointed out several features that are important to the fabrication of a calorimetric flow meter for sweat detection. By comparing theoretical calculations and COMSOL simulations, we found that the equations had failed to consider the effect of boundary conditions to the sensors. Using metal deposition to create sensors on lab-on-a-chip devices means that the sensors' height is in the nanometer range, and the sensors are essentially detecting the temperature of the boundary layer. By introducing SU-8 platforms for the sensors, we found that there is a certain platform height that would result a maximum temperature difference. Furthermore, decreasing the distance between heater and downstream sensor shows that temperature difference increase exponentially. In addition to the position of the downstream sensor, the dimensions of channel and heater temperature are also important elements that increase the temperature difference. With the same volumetric flow rate, the flow velocity is depended on the cross-sectional area of the channel. The maximum temperature difference was expected to occur at the smallest cross-sectional area, where flow velocity is the highest. However, we found that a channel height and width of approximately 3.5 mm resulted in the highest temperature difference when the platform was 100 μm and 2.85 mm away from the heater. A higher heater temperature also resulted in an increase of temperature difference, but it did not affect the relationship between temperature difference and the cross-sectional area.

As mentioned above, sweat rate analysis had begun to gain researcher's attentions [13, 14, 15]. In this paper, we proposed a new approach in sweat rate detection via thermal flow sensor. Miniaturized calorimetric flow rate sensor had been researched previously by other researchers and can measure flow rates in the order of 200-300nL/min [22, 23]. With the results of this paper, it is possible to optimize a calorimetric flow sensor for sweat rate detection and to be implemented to a wearable, electrochemical sweat sensor. We believe this paper will help researchers optimize their devices for wearable human physiology monitoring platforms.

Bibliography

[1] D.J. Casa, et. al., "National Athletic Trainers' Association Position Statement: Fluid Replacement for Athletes." *Journal of Athletic Training*. vol. 35, pp. 212–224, Apr 2000.

[2] R. Carter, S. N. Cheuvronta, D. W. Wrayb, M. A. Kolkaa, L. A. Stephensona, and M. N. Sawkaa, "The influence of hydration status on heart rate variability after exercise heat stress," *Journal of Thermal Biology*, vol. 30, issue. 7, pp. 495-502, Oct. 2005.

[3] S. N. Cheuvront, and M. N. Sawkaa, "Hydration Assessment of Athletes," *Sports Science Exchange 97*, vol. 18, no. 2, 2015.

[4] D. Morris, S. Coyle, Y. Wu, K. Lau, G. Wallace, and D. Diamond, "Bio-sensing textile based patch with integrated optical detection system for sweat monitoring," *Sensors and Actuators, B: Chemical*, vol. 139, issue. 1, pp. 231-236, May. 2009.

[5] A. J. Bandodkar, et. al., "Epidermal tattoo potentiometric sodium sensors with wireless signal transduction for continuous non-invasive sweat monitoring," *Biosensors and Bioelectronics*, vol. 54, pp. 603-609, 2014.

[6] G. Liu, et. al., "A Wearable Conductivity Sensor for Wireless Real-time Sweat Monitoring," *Sensors and Actuators B: Chemical*, to be published.

[7] T. S. Licht, M. Stern, and H. Shwachman, " Measurement of the Electrical Conductivity of Sweat Its Application to the Study of Cystic Fibrosis of the Pancreas.," *Clinical chemistry*, vol. 3, issue. 1, pp. 37-48, 1957.

[8] H. Shwachman, et. al., "ELECTRICAL CONDUCTIVITY OF SWEAT A Simple Diagnostic Test in Children," *Pediatrics*, vol. 32, issue. 1, pp. 85-88, 1963.

[9] H. Tanaka, Y. Osaka, S. Obara, H. Yamaguchi, and H. Miyamoto, "Changes in the concentrations of Na+, K+, and Cl- in secretion from the skin during progressive increase in exercise intensity," *European Journal of Applied Physiology and Occupational Physiology*, vol. 64, no. 6, pp.557-561, 1992

[10] M. J. Buono, et. al., "Sodium ion concentration vs. sweat rate relationship in humans," *Journal of Applied Physiology*. vol.103, pp.990-994, 2007.

[11] M. J. Buonoet. Al., "Na+ secretion rate increases proportionally more than the Na+ reabsorption rate with increases in sweat rate," *Journal of Applied Physiology*, vol.105, pp. 1044-1048, 2008.

[12] P. Wei, et. al., "A Conformal Sensor for Wireless Sweat Level Monitoring," *IEEE Sensors*, pp. 1-4, Nov. 2013.

[13] P. Salvo, et. al., "A Wearable Sensor for Measuring Sweat Rate," *IEEE Sensors*, vol. 10, issue. 10, pp. 1557-1558, Oct. 2010.

[14] S. Coyle, et. al., "BIOTEX-Biosensing textiles for personalized healthcare management," *IEEE Trans Inf Technol Biomed*, vol. 14, issue 2, pp. 364-370, 2010.

[15] G. Matzeu, et. al., "A Wearable Device for Monitoring Sweat Rates via Image Analysis," *IEEE Trans Biomed Eng*, 2015.

[16] J. T. W. Kuo, et. al., "Micromachined thermal flow sensors—A review," *Micromachines*, vol. 3, issue. 3, pp. 550-573, 2012.

[17] M. Elwenspoek, "Thermal flow micro sensors." in *Proc. CAS'99, IEEE Int. Conf. Semiconductor*, vol. 2, pp. 423-435.

[18] A. Arevalo, et. al., "Simulation of Thermal Transport Based Flow Meter for Microfluidics Applications," in *2013 Proc. COMSOL Conf*., Rotterdam

[19] A. Rasmussen, et. al., "Simulation and optimization of a microfluidic flow sensor," *Sensors and Actuators A: Physical*, vol. 88, pp. 121-132, 2001.

[20] N. T. Nguyen, and W. Dotzel, "Asymmetrical locations of heaters and sensors relative to each other using heater arrays: a novel method for designing multi-range electrocaloric mass-flow sensors," *Sensors and Actuators A: Physical*, vol. 62, pp. 506-512, 1997.

[21] T. S. J. Lammerink, et. al., "Integrated liquid dosing system," in *Proc. MEMS'93, IEEE*, pp 254-259.

[22] M. Dijkstra, et. al., "Miniaturized thermal flow sensor with planar-integrated sensor structures on semicircular surface channels," *Sensors and Acuators A*, vol. 143, pp. 1-6, 2008.

[23] R. Ahrens, and K. Schlote-Holubek, "A micro flow sensor from a polymer for gases and liquids," *Journal of Micromechanics and Microengineering*, vol. 19, 074006, 2009.